Synthesis, characterization and cytotoxicity of a new palladium(II) complex with a coumarine-derived ligand

ARTICLE *in* EUROPEAN JOURNAL OF MEDICINAL CHEMISTRY · MARCH 2014

Impact Factor: 3.45 · DOI: 10.1016/j.ejmech.2013.12.051

European Journal of Medicinal Chemistry 74 (2014) 502–508

Contents lists available at ScienceDirect

European Journal of Medicinal Chemistry

journal homepage: http://www.elsevier.com/locate/ejmech

Original article

Synthesis, characterization and cytotoxicity of a new palladium(II) complex with a coumarine-derived ligand

Dragoslav R. Ilić [a], Verica V. Jevtić [b], Gordana P. Radić [c], Katarina Arsikin [d], Biljana Ristić [d], Ljubica Harhaji-Trajković [e], Nenad Vuković [b], Slobodan Sukdolak [b], Olivera Klisurić [f], Vladimir Trajković [d], Srećko R. Trifunović [b,*]

[a] College of Health Studies in Ćuprija, Lole Ribara 1/2, 35230 Ćuprija, Serbia
[b] Department of Chemistry, Faculty of Science, University of Kragujevac, Radoja Domanovića 12, 34000 Kragujevac, Serbia
[c] Faculty of Medical Sciences, University of Kragujevac, Svetozara Markovića 69, 34000 Kragujevac, Serbia
[d] Institute of Microbiology and Immunology, School of Medicine, University of Belgrade, Dr. Subotica 1, 11000 Belgrade, Serbia
[e] Institute for Biological Research, University of Belgrade, Despota Stefana Blvd. 142, 11000 Belgrade, Serbia
[f] University of Novi Sad, Faculty of Sciences, Department of Physics, Trg Dositeja Obradovića 4, 21000 Novi Sad, Serbia

ARTICLE INFO

Article history:
Received 5 September 2013
Received in revised form
26 December 2013
Accepted 29 December 2013
Available online 21 January 2014

Keywords:
Coumarine-derived ligand
Palladium(II) complex
Cytotoxicity
Crystal structure
Apoptosis
Oxidative stress

ABSTRACT

The new coumarine derivative, 3-(1-(2-hydroxyethylamino)ethylidene)chroman-2,4–dione, and corresponding palladium(II) complex have been synthesized and characterized by microanalysis, infrared, ^{1}H and ^{13}C NMR spectroscopy. The proposed structure of the complex was confirmed on the basis of the X-ray structural study. The palladium(II) complex decreased viability of L929 mouse fibrosarcoma, U251 human glioma and B16 mouse melanoma cell lines in a dose dependent manner, while its ligand exhibited no significant cytotoxicity. The cytotoxic effect of the complex was comparable to that of cisplatin, and mediated by apoptosis associated with oxidative stress, mitochondrial depolarization and caspase activation. Therefore, our results indicate that newly synthesized palladium(II) complex might be a potential candidate for anticancer therapy.

1. Introduction

Coumarine and its derivatives are natural compounds with high and significant biological activities like spasmolitic, antiarrhythmic, cardiotonic and photodynamic properties [1]. Also, coumarine and its derivatives were tested against several tumor cell lines [2–4]. Some metal complexes with coumarine derivatives showed significant anticoagulant [5,6] and antitumor activity [1,7]. Also, some cerium(III), zirconium(IV), copper(II), zinc(II), bismuth(III) and cadmium(II) were significantly cytotoxic *in vitro* [8,9].

A large number of palladium(II) complexes have also been prepared and their biological activity, including anticancer properties, has been investigated [10–14], because of the structural analogy with platinum(II) complexes. The palladium(II) complexes generally showed lower antitumor activity than cisplatin, due to their more labile nature in comparison to the corresponding platinum(II) complexes [15]. However, Budzisz et al. have recently found that palladium(II) complex with 4-hydroxy-3-(1-iminoethyl)-2*H*-chromen-2-one was 7800 times more active than carboplatin [16].

Herein we describe the synthesis and characterization of the 3-(1-(2-hydroxyethylamino)ethylidene)chroman-2,4-dione and corresponding palladium(II) complex. The crystal structure of 3-(1-(2-hydroxyethylamino)ethylidene)chroman-2,4-dione-palladium(II) complex was also reported. In addition, antitumor activities of both 3-(1-(2-hydroxyethylamino)ethylidene)chroman-2,4-dione and corresponding palladium(II) complex were tested.

2. Results and discussion

2.1. Chemistry

The reaction of 3-acetyl 4-hydroxy coumarine [17] **1** with an equimolar amount of 2-aminoethanol **2** in methanol afforded product **3** in 96% yield (Scheme 1). This compound was previously

* Corresponding author. Tel.: +381 34 300263; fax: +381 34 335040.
E-mail address: srecko@kg.ac.rs (S.R. Trifunović).

0223-5234/$ – see front matter © 2014 Elsevier Masson SAS. All rights reserved.
http://dx.doi.org/10.1016/j.ejmech.2013.12.051

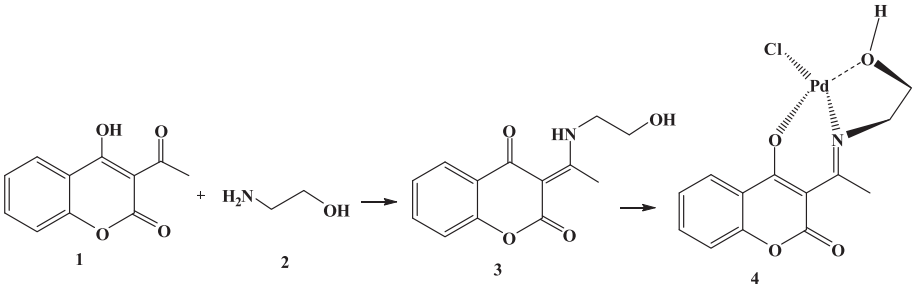

Scheme 1. Synthesis of the ligand **3** and its Pd(II) complex **4**.

synthesized by Budzisz and coworkers [18]. Spectral data of ligand 3-(1-(2–hydroxyethylamino)ethylidene)chroman-2,4-dione **3** was in accordance with literature data [18].

The structure of synthesized complex **4** was determined by means of spectral (IR, ^{1}H NMR and ^{13}C NMR) and elemental analysis, as well as X-ray diffraction study.

In comparison to IR spectral data of ligand **3**, obtained Pd complex **4** showed significant differences. The IR spectrum of Pd(II) complex **4** showed presence of Pd–O and Pd–N bands (524 cm^{-1} and 459 cm^{-1}, respectively). The band identified at 1605 cm^{-1} belongs to the imino group (C=N), while the band at 1675 cm^{-1} corresponds to coumarine lactone C=O group. These results indicated that during reaction of formation of Pd complex enamine ligand transforms to imine form. Also, it is interesting that IR spectra of complex **4** showed broadened band from OH group at 3300 cm^{-1}. At this stage we could not confirm if this band was from coumarine OH group or from hydroxy ethyl part (Table 2).

In the ^{1}H NMR spectrum of Pd complex **4**, on broadened signal at 3.40 ppm confirmed presence of OH group bonded to hydroxy ethyl part. The broadened singlet from NH group from enamine form of ligand **2** at 14.62 ppm was not observed in complex **4**. Also, exchangeable OH proton from coumarine ring is not present. The protons from CH_3–C-1′ show resonation at 2.50 ppm, which is for 0.27 ppm lower than in ligand **2**. The same situation are in the case of methylene protons from the ethyl group (CH_2–C-2″ at 3.68 ppm and CH_2–C-1″ at 3.99 ppm, respectively). All of this data confirmed that in formation of complex with Pd were involved nitrogen from imino group, oxygen bonded to coumarine part at position C-4′, as well as oxygen from hydroxyl group from hydroxy ethyl part (Table 3).

The ^{13}C NMR spectra showed signal of CH_3–C-1′ carbon at higher frequency in comparison to ligand **2** (19.6 ppm), as well as signal of carbon from C-1″ (46.6 ppm). On the other side, carbon atoms C-2″ and C-4 were observed at lower frequency than in ligand **3** (59.0 ppm and 179.5 ppm, respectively).

Table 1
Experimental details: Crystallographic data and refinement parameters.

Crystal data	
Chemical formula	$C_{13}H_{12}ClNO_4Pd$
M_r	388.09
Crystal system, space group	Orthorhombic, *Pbca*
Temperature (K)	293
a, *b*, *c* (Å)	18.373 (5), 7.324 (5), 21.280 (5)
V (Å^3)	2864 (2)
Z	8
F(000)	1536
Radiation type	Cu*Kα*
θ range (°) for cell measurement	4.8–72.0
μ (mm^{-1})	12.29
Crystal size (mm)	0.39 × 0.15 × 0.09
Data collection	
Diffractometer	Xcalibur-Gemini S diffractometer
Radiation source	Enhance (Cu) X-ray Source
Absorption correction	Gaussian *CrysAlis PRO*, Agilent Technologies, Version 1.171.36.24 (release 03-12-2012 CrysAlis171 .NET). Numerical absorption correction based on Gaussian integration over a multifaceted crystal model
T_{min}, T_{max}	0.119, 0.417
No. of measured, independent and observed [$I > 2\sigma(I)$]reflections	5983, 2553, 2191
R_{int}	0.029
θ values (°)	$\theta_{max} = 67.0$, $\theta_{min} = 4.2$
Range of *h*, *k*, *l*	$h = -10 \rightarrow 21$, $k = -8 \rightarrow 4$, $l = -24 \rightarrow 25$
Refinement	
$R[F^2 > 2s(F^2)]$, $wR(F^2)$, *S*	0.031, 0.088, 1.09
No. of reflections	2553
No. of parameters	203
H-atom treatment	H atoms treated by a mixture of independent and constrained refinement
$(\Delta/\sigma)_{max}$	0.001
$\Delta\rho_{max}$, $\Delta\rho_{min}$ (e Å^{-3})	0.54, −0.43

Computer programs: *CrysAlis PRO*, Agilent Technologies, Version 1.171.36.24 (release 03-12-2012 CrysAlis171 .NET) (compiled Dec 3 2012,18:21:49), *SHELXL97* (Sheldrick, 1997).

2.2. The crystal structure-(1-(2-hydroxyethylamino)ethylidene) chroman-2,4-dione-palladium(II) complex **4**

The perspective view of molecular structure of compound 3-(1-(2-hydroxyethylamino)ethylidene)chroman-2,4-dione-palladium(II) complex (**4**) is shown in Figs. 1 and 2 presents crystal packing for compound **4**.

From a structural point of view, one must emphasize two features of 3-(1-(2-hydroxyethylamino)ethylidene)chroman-2,4-dione-palladium(II) complex, namely, the coordination of the Pd atom and the hydrogen-bond network. The Pd atom has the usual square-planar coordination, formed here by one N, one Cl and two O atoms (Fig. 1). The main geometrical features of the PdNO2Cl group are reported in Table 4. This group is slightly distorted, but is nevertheless almost perfectly planar since the maximum displacement from the weighted least-squares plane (O1/N1/O2/Cl1) is 0.0151(3) Å for Pd atom. All other bonding parameters (Table 4) fall in the range found in the literature [19]. The crystal packing is controlled by O2–H2···O4 intermolecular contacts

Table 2
Characteristic group in the IR spectra and their wave numbers.

Compound	ν (cm^{-1})					
	NH	OH	C=O	C=N	Pd–O	Pd–N
3	3412	3380	1661	/	/	/
4	/	3300	1675	1605	524	459

Table 3
Differences of characteristic chemical shifts in ligand and Pd complex.

^{1}H NMR (200 MHz, DMSO-d_6) δ ppm		
Compound		$\Delta\delta$ ppm
3	**4**	
2.19 (br s, 1H, OH)	3.40 (br s, 1H, OH)	1.21
2.77 (s, 3H, CH_3–C-1′)	2.50 (s, 3H, CH_3–C-1′)	0.27
3.73 (t, 2H, CH_2–C-2″)	3.68 (t, 2H, CH_2–C-2″)	0.05
4.12 (t, 2H, CH_2–C-1″)	3.99 (t, 2H, CH_2–C-1″)	0.13
14.62 (br s, 1H, NH)	/	/

(geometrical details are given in Table 5). The network of "head to tail" hydrogen bonds is placed along *a* axis (Fig. 2).

2.3. The in vitro cytotoxicity of palladium(II) complex towards cancer cell lines

In order to investigate the *in vitro* anticancer activity of coumarine derivative, 3-(1-(2-hydroxyethylamino)ethylidene)chroman-2,4-dione and corresponding palladium(II) complex, mouse fibrosarcoma L929, human glioma U251 and mouse melanoma B16 cells were incubated in the presence of their various concentrations. The treatment with complex **4** for 24 h reduced the viability of all three tumor cell lines in a dose-dependent manner, as demonstrated by measuring mitochondrial dehydrogenase activity and cell membrane damage by MTT and LDH test, respectively (Fig. 3A and B). Based on the results obtained in MTT test, the IC_{50} values for complex **4** were 2.8 ± 0.8 μM, 3.3 ± 0.9 μM, and 6.9 ± 1.9 μM (mean ± SD, $n = 3$) in L929, U251 and B16 cells, respectively. The obtained IC_{50} values were slightly, but significantly lower ($p < 0.05$; *t*-test) than the corresponding IC_{50} values for the well-known anticancer drug cisplatin (10.3 ± 2.7 μM, 11.1 ± 3.2 μM, and 48 ± 9.1 μM; mean ± SD, $n = 3$). Therefore, unlike most of the recently described Pd(II) complexes [10–13], complex **4** was apparently more efficient than cisplatin, at least in the cancer cell lines tested in the present study. On the other hand, ligand **3** marginally reduced mitochondrial dehydrogenase activity in L929 and B16 cells (Fig. 3A), while failed to increase LDH release from all tumor cell lines tested (Fig. 3B). Finally, microscopic examination revealed that complex **4** caused strong vacuolization of tumor cells associated with their rounding and detachment from the cell culture plastic (Fig. 3C). Together, these results demonstrate that palladium(II) complex is toxic to against L929, U251 and B16 cancer cells.

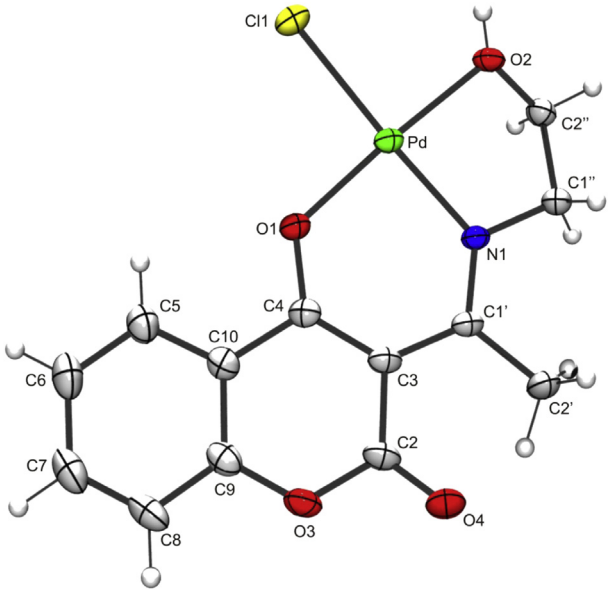

Fig. 1. Molecular structure of the complex **4** with the non-H atom numbering scheme with thermal ellipsoids at 30% probability level.

2.4. Palladium(II) complex induces apoptosis associated with oxidative stress, mitochondrial depolarization and caspase activation

We next investigated the intracellular mechanisms responsible for the cytotoxic effect of complex **4** in U251 glioma cells. Flow cytometric analysis of cell cycle demonstrated that complex **4** increased the number of apoptotic, hypodyploid cells with fragmented DNA (sub-G_0/G_1) (Fig. 4A). Accordingly, analysis of the cells stained with annexin V-FITC and propidium iodide has shown that complex **4** induced a significant increase in the numbers of both early apoptotic cells with intact cell membrane (annexin$^+$/PI$^-$), and late apoptotic cells with cell membrane damage (annexin$^+$/PI$^+$) (Fig. 4B). Palladium(II) complex-induced apoptosis was associated with activation of the principal apoptosis-executing enzymes caspases (Fig. 4C). Treatment with complex **4** caused the loss of mitochondrial membrane potential, as demonstrated by the increase in green/red (FL1/FL2) fluorescence ratio in U251 cells stained with the mitochondria-binding dye DePsipher (Fig. 4D). Using a redox-sensitive fluorochrome DCFDA, we have shown that complex **4** triggered generation of ROS (Fig. 4E), which could be at least partly attributed to superoxide, as demonstrated by staining with superoxide-selective fluorescent dye DHE (Fig. 4F). Therefore, these data indicate that palladium(II) complex induces apoptosis of cancer cells through caspase activation, mitochondrial depolarization and oxidative stress.

3. Conclusions

The prepared complex **4** has been characterized by elemental analyses, infrared and NMR (^{1}H and ^{13}C) spectroscopy. The tridentate coordination of 3-(1-(2-hydroxyethylamino) ethylidene) chroman-2,4-dione (**3**) to the palladium(II) ion, predicted on the basis of spectral data, crystallographically was confirmed. The arrangement around Pd ion, formed here by one N, one Cl and two O atoms is nevertheless almost perfectly planar. The O2–H2···O4 intermolecular contacts are responsible for crystal packing. While the ligand displays no cytotoxicity, complex **4** induces caspase-dependent apoptotic death of cancer cells, possibly mediated by oxidative stress and mitochondrial depolarization.

4. Experimental

4.1. Chemistry

4.1.1. Materials and methods

2-Aminoethanol was obtained from Acros Organics (Geel, Belgium) while methanol, ethanol, toluene and acetone were obtained from Sigma Aldrich (Munich, Germany). Compound 3-acetyl 4-hydroxy coumarine **1** was synthesized by previously described procedure [17].

Melting points were recorded on a Kofler-hot stage apparatus and are uncorrected. Microanalysis of carbon, hydrogen and nitrogen was carried out with a Carlo Erba 1106 microanalyser. The IR spectra were run on Perkin–Elmer Grating Spectrophotometers Model 137 and Model 337; KBr disc, *n* in cm^{-1}. The NMR spectra were recorded on a Varian Gemini 200 spectrometer (Varian, Palo Alto, CA); ^{1}H NMR at 200 MHz and ^{13}C NMR at 50 MHz, solvent DMSO-d_6, TMS internal standard. Chemical shifts were given in d (ppm), *J*-coupling constants in Hertz (Hz), abbreviations: s-

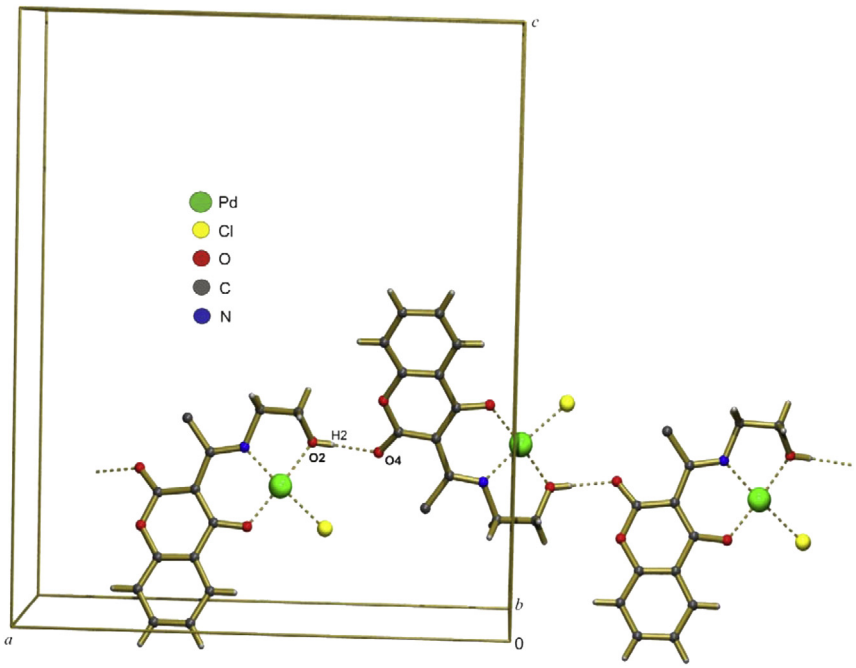

Fig. 2. PLATON drawing showing crystal packing for complex **4**. Intermolecular hydrogen bonds O2–H2···O4 are shown as dashed line.

singlet, dd-doublet of doublet, t-triplet, m-multiplet, br s-broadend singlet. Mass spectra were recorded on a 5973 mass spectrometer (Agilent, Santa Clara, CA) (MS quadruple temperature 150 °C; mass scan range, 40–600 amu at 70 eV). Analytical TLC was performed on silica gel (Silica gel 60, layer 0.20 mm, Alugram Sil G, Mashery-Nagel, Germany). Visualization of TLC plates was performed by using UV lamp at 254 nm and 365 nm (VL-4.LC, 365/254, Vilber Lourmat, France).

4.1.2. Synthesis of 3-(1-(2-hydroxyethylamino)ethylidene) chroman-2,4-dione **3**

A mixture of 3-acetyl 4-hydroxy coumarine **1** (0.4 g, 0.002 mol) and 2-aminoethanol **2** (0.12 g, 0.002 mol) in methanol (50 mL) was refluxed for 1 h. Progress of reaction was monitored by TLC (toluene:acetone = 7:3). At the end of reaction, the solvent was evaporated to one quarter of its volume; then the obtained white crystals were filtered, dried and recrystallized from 96% ethanol. Yield: 0.48 g (97%), mp: 181–183 °C. Anal. calcd. for $C_{13}H_{13}NO_4$ (M_r = 247.25 g/mol) (%): C, 63.15; H, 5.30; N, 5.67. Found: C, 62.78; H, 5.10; N, 5.87.

IR (KBr, in cm^{-1}) 3412 (NH), 3300 (OH), 3050 (=CH), 2948, 2894 (CH), 1661 (C=O from 2,4-dioxochroman part), 1615, 1592, 1573 and 1487 (C=C)$_{ar}$ cm^{-1};

^{1}H NMR (200 MHz, DMSO-d_6) δ ppm: 2.19 (br s, 1H, OH), 2.77 (s, 3H, CH_3–C-1′), 3.73 (t, 2H, CH_2–C-2″, ^3J = 5.8 Hz), 4.12 (t, 2H, CH_2–C-1″, ^3J = 5.8 Hz), 7.18 (2H, m, C–H-6, C–H-7), 7.55 (1H, dd, $^3J_{H\text{-}8,\ H\text{-}7}$ = 8.10 Hz, $^4J_{H\text{-}8,\ H\text{-}6}$ = 2.11 Hz, C–H-8), 8.05 (1H, dd, $^3J_{H\text{-}5,\ H\text{-}6}$ = 7.99 Hz, $^4J_{H\text{-}5,\ H\text{-}7}$ = 1.90 Hz, C–H-5), 14.62 (br s, 1H, NH);

^{13}C NMR (200 MHz, DMSO) δ ppm: 18.9 (C-1′–CH_3), 46.2 (C-1″), 60.5 (C-2″), 97.4 (C-3), 116.6 (C-8), 120.6 (C-6), 123.6 (C-5), 126.0 (C-10), 133.8 (C-7), 152.2 (C-9), 153.7 (C-2), 177.1 (C-1′), 181.3 (C-4).

MS *m*/*z* (%): 247 (M^+, 100), 216 (8), 204 (72), 187 (63), 175 (12), 147 (19), 121 (52), 92 (34), 67 (27).

Table 4
Selected geometrical parameters for 3-(1-(2-hydroxyethylamino)ethylidene)chroman-2,4-dione-palladium(II) complex **4**.

Bond lengths [Å]	
Pd–O1	1.950 (3)
Pd–N1	1.974 (3)
Pd–O2	2.018 (3)
Pd–Cl1	2.3069 (11)
Bond angles [°]	
O1–Pd–N1	93.30 (13)
O1–Pd–O2	176.33 (12)
N1–Pd–O2	83.17 (13)
O1–Pd–Cl1	90.00 (9)
N1–Pd–Cl1	176.61 (10)
O2–Pd–Cl1	93.52 (9)
C2″–O2–Pd	106.2 (2)
C4–O1–Pd	124.7 (3)
C1′–N1–Pd	126.6 (3)
C1″–N1–Pd	111.3 (2)
Torsion angles [°]	
Pd–O1–C4–C3	1.5 (6)
Pd–O1–C4–C10	−179.1 (3)
Pd–N1–C1″–C2′	−18.0 (5)
Pd–N1–C1′–C3	7.3 (6)
Pd–N1–C1′–C2′	−177.3 (3)
Pd–O2–C2″–C1″	−50.4 (4)

4.1.3. Synthesis of 3-(1-(2-hydroxyethylamino)ethylidene) chroman-2,4-dione-palladium(II) complex **4**

K_2PdCl_4 (0.0652 g, 0.2 mmol) was dissolved in 10.0 mL of water on steam bath and equimolar amount of the 3-(1-(2-hydroxyethylamino)ethylidene)chroman-2,4-dione (0.0495 g, 0.2 mmol), dissolved in methanol (12.0 mL), was added. The mixture was stirred for 48 h and yellow precipitate was obtained. The precipitate was filtered off and filtrate was left over several days and produced crystals suitable for X-ray measurement. Yield:

Table 5
Hydrogen bonding geometry for complex **4**.

D–H···A	D–H (Å)	H···A (Å)	D···A (Å)	θ (°)
O2–H2···O4[a]	0.74(6)	1.84(5)	2.575(5)	171(6)

[a] $-1/2 + x, y, 1/2 - z$.

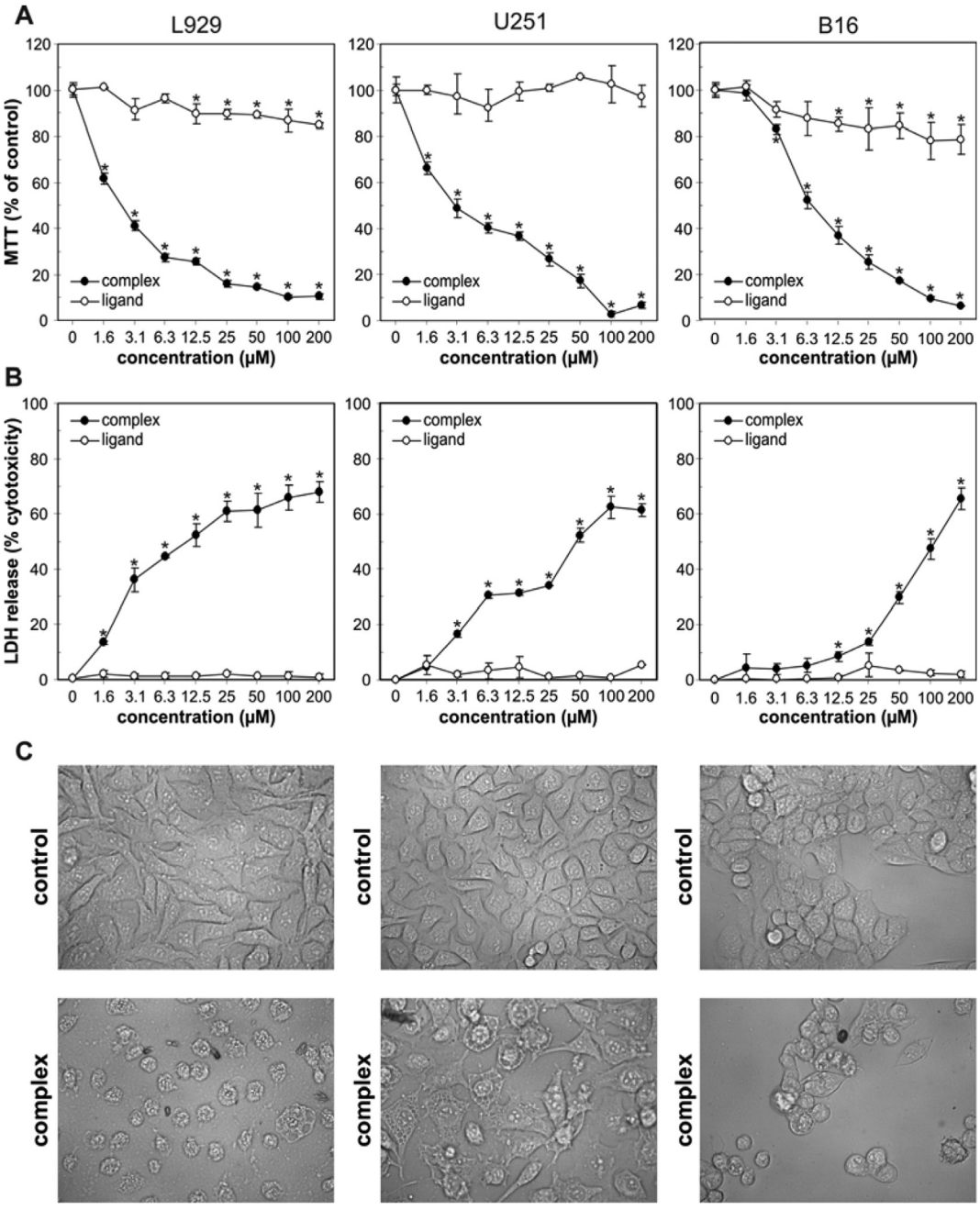

Fig. 3. Complex **4** is toxic to L929, U251 and B16 cancer cells. (A, B) L929, U251 and B16 cells were incubated for 24 h with complex **4** or ligand **3**. Cell viability was determined by MTT (A) or LDH release test (B). The data are mean ± SD values of triplicates from a representative of three independent experiments ($p < 0.05$* compared to untreated control). (C) Cell morphology of untreated cells or cells treated with 6.25 μM of complex **4** was assessed by optical microscopy (C).

0.051 g (65.7%). Anal. calcd. for $C_{13}H_{12}ClNO_4$ (M_r = 388.106 g/mol) (%): C, 41.23; H, 3.12; N, 3.61. Found: C, 41.32; H, 3.97; N, 3.88.

IR (KBr, n in cm^{-1}) 3425 (OH), 3067 and 3035 (=CH), 2922, 2898, 2852 and 2818 (CH), 1675 (C=O), 1605 (C=N), 1601, 1570 and 1482 $(C{=}C)_{ar}$, 524 (Pd–O), 459 (Pd–N);

^{1}H NMR (200 MHz, DMSO-d_6) δ ppm: 2.50 (s, 3H, CH_3–C-1′), 3.40 (br s, 1H, OH), 3.68 (t, 2H, CH_2–C-2″, ^3J = 5.3 Hz), 3.99 (t, 2H, CH_2–C-1″, ^3J = 5.3 Hz), 7.27 (2H, m, C–H-6, C–H-7), 7.59 (1H, dd, $^3J_{H\text{-}8,\ H\text{-}7}$ = 8.10 Hz, $^4J_{H\text{-}8,\ H\text{-}6}$ = 2.11 Hz, C–H-8), 7.93 (1H, dd, $^3J_{H\text{-}5,\ H\text{-}6}$ = 7.99 Hz, $^4J_{H\text{-}5,\ H\text{-}7}$ = 1.90 Hz, C–H-5);

^{13}C NMR (200 MHz, DMSO) δ ppm: 19.6 (C-1′–CH_3), 46.6 (C-1″), 59.0 (C-2″), 96.2 (C-3), 116.2 (C-8), 120.4 (C-6), 123.7 (C-5), 125.7 (C-10), 133.6 (C-7), 152.6 (C-9), 153.1 (C-2), 176.3 (C-1′), 179.5 (C-4). Both ligand **3** and complex **4** and were stored at +4 °C as 100 mM stock solutions in dimethyl sulfoxide (DMSO), and were diluted in culture medium immediately before use.

4.2. Structure determination

A single crystal of 3-(1-(2-hydroxyethylamino)ethylidene) chroman-2,4-dione-palladium(II) complex was selected and mounted on a glass fiber. Diffraction data were collected using the Oxford Diffraction Gemini S four-circle goniometer equipped with Sapphire CCD detector. The crystal to detector distance was

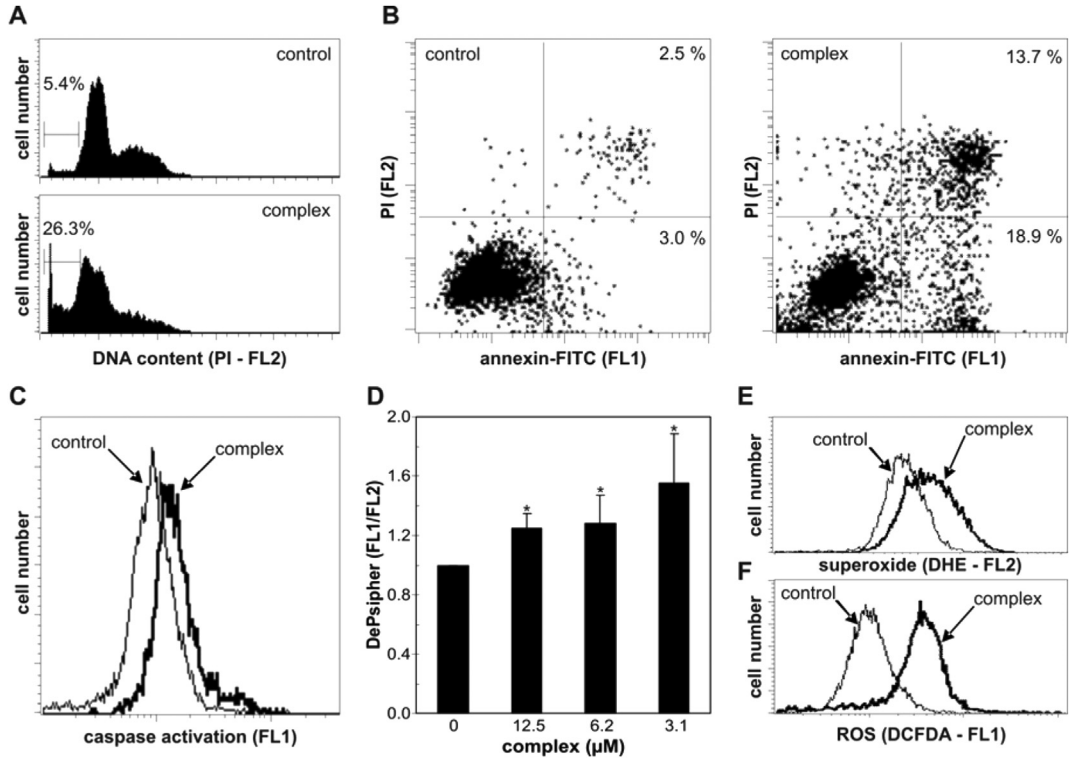

Fig. 4. Complex **4** induces apoptosis associated with oxidative stress, mitochondrial depolarization and caspase activation. U251 cells were incubated in the absence or presence of 6.25_M (A-C, E-F) or various concentrations of complex **4** (D). After 24 h, the cells were stained with PI (A) or annexin-FITC/PI (B), and the flow cytometric analysis of DNA fragmentation (A) or phosphatidylserine externalization (B) were performed. Alternatively, cells were stained with ApoStat (C), DePsipher (D), DHE (E) or DCFDA (F) and caspase activation (C), mitochondrial depolarization (D), superoxide production (E) or total ROS production (F) was examined by flow cytometry after 16 h of incubation. The representative dot plots and histograms from at least three experiments are presented in (A–C, E–F), while the data in (D) are mean + SD values from three independent experiments ($p < 0.05^*$ compared to untreated control).

45.0 mm and graphite monochromated CuKα ($\lambda = 1.5418$ Å) radiation was used for the experiments. The data were reduced using the program CrysAlis PRO [20]. A numerical absorption correction based on Gaussian integration over a multifaceted crystal model was applied, and the data were corrected for Lorentz, polarization, and background effects [20]. The structure was solved by direct methods using Sir 97 program [21] and refined by full-matrix least-squares procedures on F^2 using SHELXL-97 programs [22] as implemented in the WinGX program suite [23]. The non-H atoms were refined anisotropically. The positions of hydrogen atoms were found from the inspection of the difference Fourier maps. At the final stage of the refinement, H atoms from the methyl group and aromatic ring were positioned geometrically (C–H = 0.96 Å and C–H = 0.93 Å, respectively) and refined using a riding model with fixed isotropic displacement parameters. Crystallographic data and refinement parameters are listed in Table 1. The figures representing molecular structure were made using ORTEP-3 [24] and PLATON [25] programs.

4.3. Biology

4.3.1. Cells and reagents

All reagents were purchased from Sigma (St. Louis, MO), unless stated otherwise. The human glioma cell line U251 was kindly donated by Dr. Pedro Tranque (Universidad de Castilla–La Mancha, Albacete, Spain), while the mouse B16 melanoma cell line and the mouse fibrosarcoma cell line L929 were obtained from the European Collection of Animal Cell Cultures (Salisbury, UK). The tumor cell lines were maintained at 37 °C in a humidified atmosphere with 5% CO_2, in a RPMI cell culture medium (PAA Laboratories, Pasching, Austria) supplemented with 5% fetal calf serum (FCS) and penicillin/streptomycin. The cells were prepared for experiments using the conventional trypsinization procedure with trypsin/EDTA and incubated in 96-well flat-bottom plates (1×10^4 cells/well) for the cell viability assessment, or 24-well plates (5×10^4 cells/well) for the flow cytometric analysis. Cells were rested for 24 h then treated with complex or ligand, as described in Results and Figure legends.

4.3.2. Determination of cell viability

MTT [3-(4,5-dimethylthiazol-2-yl)-2,5-diphenyltetrazolium bromide] and lactate dehydrogenase (LDH) release assays were used to assess mitochondrial dehydrogenase activity and cell membrane integrity, respectively, as markers of cell viability. The tests were performed exactly as previously described [26]. The results were presented as % of the control viability (MTT) arbitrarily set to 100%, or as % of cytotoxicity (LDH), using Tryton X-100-lysed untreated cells as a positive control. The IC_{50} values were calculated using GraphPad Prism software.

4.3.3. DNA fragmentation and apoptosis/necrosis analysis

DNA fragmentation was analyzed by flow cytometry using a DNA-binding dye propidium iodide (PI) as previously described [26]. Apoptotic/necrotic cell death was analyzed by flow cytometry following double staining with annexin V-FITC and PI, in which annexin V binds to apoptotic cells with exposed phosphatidylserine, while PI labels the necrotic cells with membrane damage. Staining was performed according to the instructions by the manufacturer (BD Pharmingen, San Diego, CA). A green/red (FL1/FL2) fluorescence of annexin/PI- and PI-stained cells was analyzed with FACSCalibur

flow cytometer (BD, Heidelberg, Germany). The numbers of viable (annexin$^-$/PI$^-$), early apoptotic (annexin$^+$/PI$^-$) and late apoptotic (annexin$^+$/PI$^+$) cells, as well as the proportion of hypodyploid, apoptotic cells with fragmented DNA (sub-G compartment) were determined using a Cell Quest Pro software (BD).

4.3.4. Caspase activation

Activation of caspases was measured by flow cytometry after labeling the cells with a cell-permeable, FITCconjugated pan-caspase inhibitor (ApoStat; R&D Systems, Minneapolis, MN) according to the manufacturer's instructions. The increase in green fluorescence (FL1) as a measure of caspase activity was determined using FACSCalibur flow cytometer.

4.3.5. Mitochondrial membrane potential measurement

Mitochondrial membrane potential was assessed using DePsipher (R&D Systems, Minneapolis, MN), a lipophilic cation that has the property of aggregating upon membrane polarization forming an orange–red fluorescent compound. If the potential is disturbed, the dye cannot access the transmembrane space and remains or reverts to its green monomeric form. The cells were stained with DePsipher as described by the manufacturer, and the green monomer and the orange–red aggregates were detected by flow cytometry. The decrease in orange/green fluorescence ratio (FL2/FL1) reflects mitochondrial depolarization.

4.3.6. Reactive oxygen species (ROS) determination

Intracellular production of ROS was determined by measuring the intensity of green fluorescence emitted by the redox-sensitive dye 2′,7′-dichlorofluorescein diacetate (DCFDA), while superoxide generation was measured using dihydroethidium (DHE) (both from Life Technologies, Carlsbad, CA), according to the manufacturer's instructions. The mean intensity of green (FL1 – DCFDA) or red (FL2 – DHE) fluorescence, corresponding to total ROS or superoxide levels, respectively, was determined using a FACSCalibur flow cytometer.

4.3.7. Statistical analysis

The statistical significance of the differences between treatments was assessed using a *t*-test or one-way ANOVA followed by Student–Neuman–Keuls test for multiple comparisons. A value of $p < 0.05$ was considered significant.

Acknowledgments

The authors are grateful to the Ministry of Education, Science and Technological Development of the Serbia (Projects No. OI172016, OI172021, III41025) and Research Center of Serbian Academy of Arts and Sciences and the University of Kragujevac for financial support.

Appendix A. Supplementary data

Supplementary data related to this article can be found at http://dx.doi.org/10.1016/j.ejmech.2013.12.051.

References

[1] I. Manolov, I. Kostova, T. Netzeva, S. Konstantinov, M. Karaivanova, Arch. Pharm. Pharm. Med. Chem. 333 (2000) 93–98.
[2] U.S. Weber, B. Steffen, C. Siegers, Res. Commun. Mol. Pathol. Pharmacol. 99 (1998) 193.
[3] D. Egan, P. James, D. Cooke, R. O'Kennedy, Cancer Lett. 118 (1997) 201–211.
[4] F. Rosskopt, J. Kraus, G. Franz, Pharmazie 47 (1992) 139–142.
[5] D. Jiang, R. Deng, J. Wu, Wuji Huaxue 5 (1989) 21–28.
[6] R. Deng, J. Wu, L. Long, Bull. Soc. Chim. Bell 101 (1992) 439–443.
[7] I. Kostova, I. Manolov, T. Netzeva, S. Konstantinov, M. Karaivanova, Eur. J. Med. Chem. 34 (1999) 63–68.
[8] I. Kostova, I. Manolov, T. Netzeva, M. Karaivanova, Arch. Pharm. Pharm. Med. Chem. 334 (2001) 157–162.
[9] M. Karaivanova, I. Manolov, M.L. Ninassyan, N.D. Danchev, S.M. Samurova, Pharmazie 49 (1994) 856–857.
[10] E. Gao, L. Liu, M. Zhu, Y. Huang, F. Guan, X. Gao, M. Zhang, L. Wang, W. Zhang, Y. Sun, Inorg. Chem. 50 (2011) 4732–4741.
[11] M. Juribašić, K. Molčanov, B. Kojić-Prodić, L. Bellotto, M. Kralj, F. Zani, L.J. Tušek- Božić, Inorg. Biochem. 105 (2011) 867–879.
[12] J. Zhang, L. Li, L. Ma, F. Zhang, Z. Zhang, S. Wang, Eur. J. Med. Chem. 46 (2011) 5711–5716.
[13] J. Quirante, D. Ruiz, A. Gonzalez, C. López, M. Cascante, R. Cortés, R. Messeguer, C. Calvis, L. Baldomà, A. Pascual, Y. Guérardel, B. Pradines, M. Font-Bardía, T. Calvet, C. Biot, J. Inorg. Biochem. 105 (2011) 1720–1728.
[14] P. Kalaivani, R. Prabhakaran, F. Dallemer, P. Poornima, E. Vaishnavi, E. Ramachandran, V.V. Padma, R. Renganathan, K. Natarajan, Metallomics 4 (2012) 101–113.
[15] E.R. Jamieson, S.J. Lippard, Chem. Rev. 99 (1999) 2467–2498.
[16] (a) E. Budzisz, B.K. Keppler, G. Giester, M. Wozniczka, A. Kufelnicki, B. Nawrot, Eur. J. Inorg. Chem. (2004) 4412–4419;
(b) E. Budzisz, U. Krajewska, M. Rozalski, Pol. J. Pharmacol. 56 (2004) 473–478.
[17] S. Sukdolak, N. Vuković, S. Solujić, N. Manojlović, Lj. Krstić, J. Heterocycl. Chem. 41 (2004) 593–596.
[18] E. Budzisz, E. Brzezinska, U. Krajewska, M. Rozalski, Eur. J. Med. Chem. 38 (2003) 597–603.
[19] F.H. Allen, O. Kennard, D.G. Watson, L. Brammer, A.G. Orpen, R. Taylor, Chem. Soc. Perkin Trans. II (1987) S1–S19.
[20] Agilent, CrysAlis PRO, Agilent Technologies, Yarnton, Oxfordshire, England, 2010.
[21] (a) A. Altomare, M.C. Burla, M. Cavalli, G. Cascarano, C. Giacovazzo, A. Gagliardi, A.G. Moliterni, G. Polidori, R. Spagna, Sir97: a New Program for Solving and Refining Crystal Structures, Istituto di Ricerca per lo Sviluppo di Metodologie Cristallografiche CNR, Bari, 1997;
(b) A. Altomare, M.C. Burla, M. Cavalli, G. Cascarano, C. Giacovazzo, A. Gagliardi, G.G. Moliterni, G. Polidori, R. Spagna, J. Appl. Crystallogr. 32 (1999) 115.
[22] G.M. Sheldrick, SHELXS-97 and SHELXL-97. Programs for Solution and Refinement of Crystal Structures from Diffraction Data, University of Göttingen, Germany, 1997. Acta Crystallogr. (A64) (2008) 112.
[23] L.J. Farrugia, WinGX, University of Glasgow, Scotland, 1998. J. Appl. Crystallogr. (32) (1999) 837.
[24] L.J. Farrugia, ORTEP-3 for Windows, University of Glasgow, Scotland, 1997. J. Appl. Crystallogr. (30) (1997) 565.
[25] A.L. Spek, Acta Crystallogr. D65 (2009) 148.
[26] G.N. Kaluđerović, D. Miljković, M. Momčilović, V.M. Đinović, M. Mostarica Stojković, T.J. Sabo, V. Trajković, Int. J. Cancer 116 (2005) 479–486.